ATMOSPHERIC SCIENCE LETTERS
Atmos. Sci. Let. **16**: 228–233 (2015)
Published online 1 December 2014 in Wiley Online Library
(wileyonlinelibrary.com) **DOI:** 10.1002/asl2.544

RMetS
Royal Meteorological Society

Contribution of coherent structures to the buoyancy heat flux under different conditions of stationarity over Amazonian forest sites

Marcelo Zeri,[1]* Leonardo Deane A. Sá[2] and Carlos A. Nobre[3]
[1] *Brazilian Center for Monitoring and Early Warnings of Natural Disasters (CEMADEN), São José dos Campos, SP, Brazil*
[2] *Centro Regional da Amazônia, Instituto Nacional de Pesquisas Espaciais, Belém, PA, Brazil*
[3] *Secretaria de Políticas e Programas de Pesquisa e Desenvolvimento, Ministério da Ciência Tecnologia e Inovação, Brasília, DF, Brazil*

Correspondence to: M. Zeri, Brazilian Center for Monitoring and Early Warnings of Natural Disasters (CEMADEN), Estrada Doutor Altino Bondesan, 500 – Eugênio de Melo, 12247–016, São José dos Campos, SP, Brazil. E-mail: marcelo.zeri@cemaden.gov.br

Received: 2 July 2014
Revised: 8 October 2014
Accepted: 13 October 2014

Abstract

The contribution of coherent structures (CSs) to daytime buoyancy heat flux was calculated for three forest sites in the Amazon region and a wetland site. Ejections and sweeps had similar contributions to fluxes at all sites, and when decomposing this contribution in scales, the resulting spectra were narrower for the forests. When accounting for times scales from 10 to 200s, CSs contributed to approximately 80% of fluxes for Caxiuanã forest site, with lower values for other locations. Among the forest, the contribution for the Jaru site was the lowest (≈66%) due to peak of contribution being close to 200s.

Keywords: turbulence; coherent structures; eddy covariance method; wavelet analysis; Pantanal wetland; Amazon forest

1. Introduction

Global climate models of the exchanges of heat, mass and energy between the atmosphere, oceans and the biosphere take into account different scales in the temporal and spatial domains. Large-scale circulations (meridional or zonal) account for most of the exchanges of heat and mass between different layers of the troposphere and the terrestrial surface, while circulations in the ocean account for the transport between the equator and the poles (Hartmann, 1994). To investigate the interaction between the troposphere and the terrestrial vegetation in finer spatial scales, so that cloud formation processes are known, for example, it is then required that different methodologies are used to estimate the exchanges of energy and mass in the atmospheric boundary layer, the lower part of the troposphere. The exchanges of energy and mass in the boundary-layer are mostly associated with eddies of different sizes, and the turbulent fluxes associated with them. The characterization of such motions and fluxes is crucial to the parameterization of global climate models or the so-called large-eddy simulations, examples of methodologies that expand the knowledge of fluxes over larger spatial scales.

Coherent structures over plant canopies are manifestations of organized eddies that are part of the flow over forests and other kinds of vegetated surfaces (Raupach and Thom, 1981; Raupach *et al.*, 1996; Finnigan, 2000). Coherent motions are assumed to be caused by instabilities in the flow over the canopy, which are related to the vertical profile of wind speed (Brunet and Irvine, 2000). This profile has an inflection point just above the canopy top separating two layers of the flow with different wind speed. The height of the inflection point over Amazon forest sites was reported before as changing during the day (Sá and Pacheco, 2006) and to modulate the duration of coherent structures (Dias Júnior *et al.*, 2013).

During the last decades, the contribution of such organized features to the vertical fluxes of scalars or energy was calculated over many different vegetated surfaces. While a major – 80% or more – contribution to fluxes is reported in some works (Bergstrom and Hogstrom, 1989; Gao *et al.*, 1989 Hogstrom and Bergstrom, 1996), other experiments and data analysis result in a lower fraction – 40% – of fluxes associated with the organized motions passing over the canopy (Lu and Fitzjarrald, 1994). In addition, other works report that different methods of detection or accounting of coherent motions might result in different contributions to fluxes (Thomas and Foken, 2007; Zeri and Sá, 2011a). In this work, we report on the contribution of coherent structures over four sites: one in a wetland region, already described in Zeri and Sá (2011a), and three forest sites in the Amazon (Jaru, Manaus and Caxiuanã).

The results were also analyzed in context to the level of stationarity found in each site. The stationarity is important so that coherent structures are well defined, besides being a key component among the factors influencing the contribution of organized motions to fluxes. In fact, Li and Fu (2013) used the Telegraph Approximation (TA) method to quantify the effects of nonstationarity (NS) on clustering of turbulence on time series of vertical velocity. The authors found that, under conditions with high NS, large-scale structures are more frequent in the time series, which could be caused by the stable stratification, gravity waves, or vertical wind shear, as suggested also by Mahrt (2011). Turbulence under very stable stratification regimes can be caused by wave motions (Mahrt, 2011), while small sub-mesoscale motions, with time scales of a few minutes, make it difficult to establish an equilibrium between turbulence and the influence of NS (Conangla *et al.*, 2008). This could generate an interaction between large and small scales, causing NS in certain scales of motion, such as the typical duration of coherent structures. Large-scale motions generate intermittency in the time series, with calm periods followed by strong turbulent activity and large departures from the mean. Thus, periods with high levels of intermittency and NS will likely be associated with coherent structures with longer time scales.

2. Site and data

The analysis was applied to four datasets: three of them from forest sites in the Amazon and one from a wetland site in the Pantanal region, Brazil (Figure 1 and Table 1). The first forest site was located in the Jaru Biological Reserve, in the southwestern part of the Amazon. Measurements were carried out using a three-dimensional (3D) sonic anemometer (model Solent 1012R2; Gill Instruments, UK), installed at 63.4 m and operating at 10.4 Hz. This site will be referred as Jaru63_dry. The second forest site was located within the Cuieiras Reserve, near the city of Manaus, AM. The dataset from this site will be referred as Manaus_dry. Measurements were carried out on a 50-m tall tower mounted on a plateau, with an eddy covariance system installed at 53.1 m. The sonic anemometer (model Solent 1012R2; Gill Instruments, UK) was set to record at 10 Hz. The third forest site is called Caxiuana_dry – and it was located inside a national reserve in the state of Pará, northeast of the Amazon region. Measurements were taken at 57 m above the canopy using a 3D sonic anemometer (model CSAT3, Campbell Scientific, Utah, USA) operating at 20 Hz. At all forest sites, canopy height was reported to be ≈35 m, with some trees reaching up to 50 m. Additional information about Amazonian sites is described in Andreae *et al.* (2002). The wetland site was located in the Pantanal region, western Brazil, in the state of Mato Grosso do Sul. The measurement site is located at the southern region of Pantanal wetland, near the city of Corumbá. The vegetation is typical of the savannah, composed of shrubs and sparsely covered by trees that are ≈16 m high. Data were collected using a 3D sonic anemometer (model CSAT3; Campbell Scientific, Inc., Utah, UT, USA) operating at 16 Hz. Detailed information about all sites can be seen in Table 1.

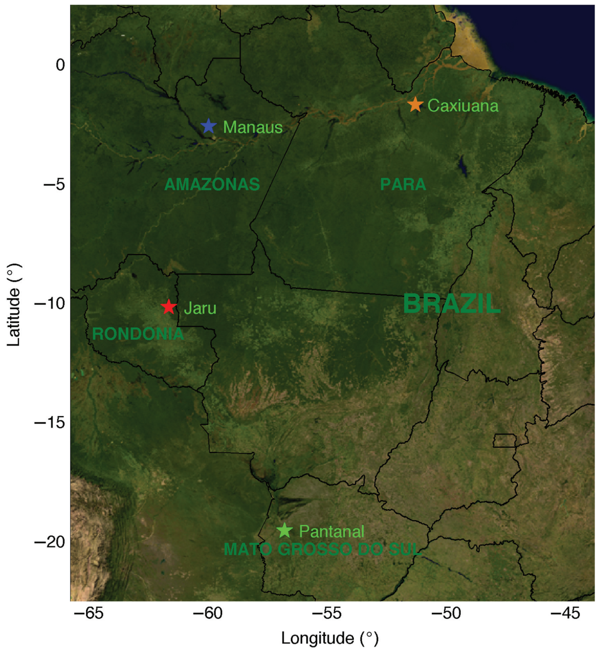

Figure 1. Site locations over the Amazon region. Picture in the background from composite of Terra/MODIS sensor and USGS topography data (http://visibleearth.nasa.gov/).

3. Methodology

Buoyancy heat flux was calculated using the eddy-covariance technique. The coordinate system was rotated using a two-dimensional (2D) scheme, where the horizontal components of wind velocity are aligned with the main wind direction and the vertical component is forced to zero (Kaimal and Finnigan, 1994). The planar-fit scheme for coordinate rotation was not used here as long-term time series of wind speed were not available to obtain the rotation factors with confidence (Lee, 1998; Wilczak *et al.*, 2001). For this reason, the 2D rotation was used for all sites. Sensible heat flux is calculated as $H = \rho c_p \overline{w'T'}$, where ρ is the air density, c_p is the specific heat of air, and w' and T' are deviations from the mean for the vertical velocity and air temperature, respectively. No direct high-frequency measurements of water vapor were available for the Pantanal site. For that reason, temperature and kinematic fluxes could not be corrected for the effects of air humidity and density (Webb *et al.*, 1980; Schotanus *et al.*, 1983). Hence, the heat flux will be referred to as the buoyancy heat flux, as the sonic temperature is approximately equal to the virtual temperature (Kaimal and Gaynor, 1991; Liu and Foken, 2001). High frequency measurements of water vapor at the forest sites were not used so that the same methodology applied to Pantanal could be used at all sites.

Stationarity of time series is a fundamental requirement when measuring fluxes using instruments fixed on a tower, just like the eddy covariance method. The flow should not change substantially when passing by the tower, so that Taylor's 'frozen turbulence' hypothesis is valid, i.e. measurements taken on a fixed location

Table 1. Information on sites, data and measurements.

Site	Location	Altitude (m, above sea level)	Canopy height (m)	Measurement height (m)	Period of data
Jaru	10°11′21.27″S, 61°52′15.17″W	145	35	63.4	Sep–Nov, 2002
Pantanal	19°34′S, 57°01′W	80	16	21.0	Jul–Nov, 2002
Manaus	2°36′32.67″S, 60°12′33.48″W	130	35	53.1	Jul–Sep, 2011
Caxiuanã	1°42′30″S, 51°31′45″W	62	32	57.0	Jul–Sep, 2005

are representative of the flow passing over the surface (Stull, 1988). The stationarity of a time series is a measure of how the statistical moments (mean, variance, skewness) change over time during a certain period (Wilks, 1995). The rate of stationarity can be calculated in many ways, such as in Cava *et al.* (2014) or Mahrt (1998), but the comparison between methods goes beyond the scope of this paper. Stationarity in this work was calculated by dividing a time series x into blocks of 5 min, then calculating 5-min means and averaging them into BA, i.e. the average of all blocks (Foken and Wichura, 1996; Vickers and Mahrt, 1997). This average is then compared with the total average of the time series, TA. When the ratio BA/TA is close to unity, then short-term variability is small and the series is considered stationary. When BA/TA deviates from unity, variability in the small blocks reduces the stationarity of the time series.

The contribution of ejections and sweeps to the heat flux was calculated using the quadrant analysis, a method where the flux is calculated using the departures of vertical velocity, w', and temperature, T', located in specific quadrants of a $w-T$ scatter plot (Wallace *et al.*, 1972; Gao *et al.*, 1989; Thomas *et al.*, 2008). In this method, ejections are associated with positive w' and sweeps with negative w'. In combination with the sign of T', some quadrants are associated with warm updrafts ($w' > 0$, $T' > 0$) or cold downdrafts ($w' < 0$, $T' < 0$). The flux of heat associated with warm or cold events is then calculated using only the departures in the respective quadrants. In this work, the fractions of sweeps and ejections were calculated for different time scales by decomposing the signals of w and T using wavelet analysis, and then performing the quadrant analysis for each scale.

Wavelet analysis has been used in many publications in the last decades as it provides a unique way of visualizing the different harmonics, or frequencies, in time series (Daubechies, 1992; Farge, 1992). The method is recommended for time series with non-periodic events, such as the turbulent motions over forests. Applications included analysis of time series of climatology (Torrence and Compo, 1998), the investigations of the time scales of turbulence and wavelike motions over forests (Collineau and Brunet, 1993; Thomas and Foken, 2005; Zeri and Sá, 2011c), and applications to time series of river levels (Sá *et al.*, 1998). The signals of vertical velocity and air temperature were decomposed using orthogonal wavelets (using the Daubechies mother wavelet), which are fast for processing long time series as they use a limited number of discrete levels. The scripts used were available from the Wavelab toolbox for MATLAB (The Mathworks Inc.; http://www-stat.stanford.edu/~wavelab/).

4. Results

Stationarity of time series is essential for flux calculation and other methodologies, such as surface renewal analysis (Foken and Wichura, 1996; Spano *et al.*, 2000; Durden *et al.*, 2013; Zeri *et al.*, 2013; Cava *et al.*, 2014). Stationarity of air temperature was estimated for all sites to assess its influence on the contribution of coherent structures to the heat flux. The level of stationarity for the temperature signal had a well-defined daily cycle and differed significantly among the four sites (Figure 2). In general, stationarity dropped during the sunrise and sunset transitions, as expected, when the surface heating or radiative cooling – which are nonstationary forcings by nature – create local circulations, such as valley-crest wind flows or drainage of cold air down the slopes of the terrain. The Caxiuanã site had the highest level of stationarity, during daytime or nighttime. The tower is located near the Caxiuanã Bay, and the flow associated with the water breezes is homogeneous, although short episodes of downbursts were already reported for this site (Nogueira *et al.*, 2006). The second best site for stationarity of air temperature was the Pantanal wetland, most likely due to the homogeneous flow over the flat terrain around the tower. In addition, measurements at this site were carried out at 21 m, much higher than the average height of the sparse vegetation in the area (~4 m), and thus less disturbed by the downbursts and outbursts to and from the canopy space.

The sites with the lowest levels of stationarity were Jaru and Manaus. The stationarity of the horizontal wind speed (not shown) was also the lowest for the Jaru site, when compared with other sites in the Amazon (Zeri *et al.*, 2013). Additionally, results reported before using data from a tower on a different location within the Jaru Reserve have indicated the influence of low frequency motions on the variances and fluxes (von Randow *et al.*, 2002, 2006). The Manaus site is located over an undulating terrain, and the valleys and peaks contribute to drainage flow during the night and horizontal advection during windy conditions (Araujo *et al.*, 2002; de Araújo *et al.*, 2010). The characteristics of the terrain are thus favorable to the existence of local

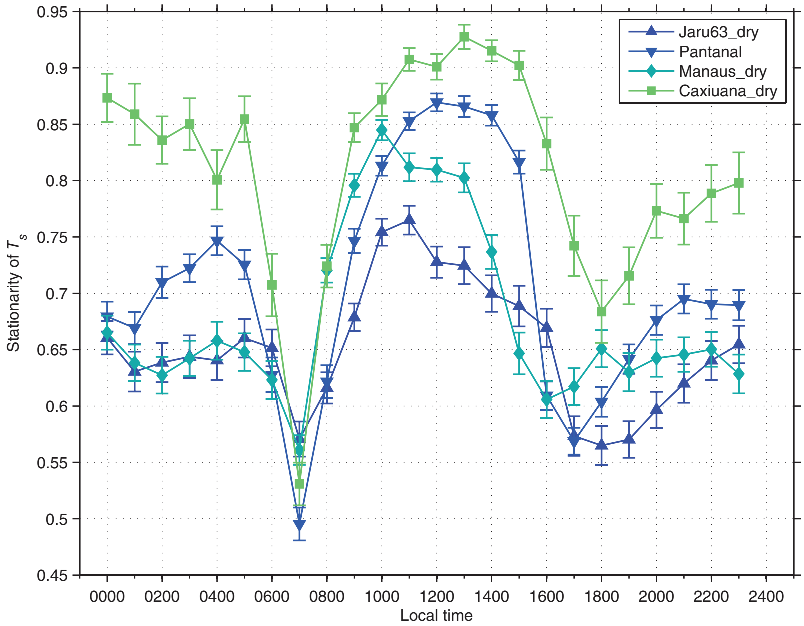

Figure 2. Daily cycle of stationarity of air temperature measured by the sonic anemometer. With the exception of the dataset for Pantanal, part of the results in this figure was already presented in Zeri *et al.* (2013). Here, only the dry seasons are shown.

circulations that disturb the flow over the canopy and the stationarity of time series, fluxes and variances.

The contribution of coherent structures to the daytime heat flux is shown in Figure 3, with cumulative sums on the right column. The shape of the spectra was the same for ejections (a) and sweeps (c) for the same sites. While the spectra for ejections and sweeps was broader for Pantanal, Caxiuanã and Manaus had narrow spectra with peaks around 50 s. However, the peak for Jaru was around 200 s, in agreement with the occurrence of low frequency motions at this site. The cumulative contribution of ejections and sweeps [panels (b) and (d)] accounted together result in approximately 90–100% of the flux (first row in Table 2). When the cumulative sums are considered from the range of 0 to 100 s only, the typical time scale of a coherent structure, the organized motions account for ≈80% of the heat flux, for the forest site of Caxiuanã, followed by Manaus, Jaru (70 and 66%) and Pantanal (55%). The lowest value for Pantanal might be attributed to the stronger contribution of high frequency fluctuations, with scales lower than 10 s. Measurements at the site were made at 21 m, which is approximately twice the average height of the vegetation at the site. According to the 'family portrait' of turbulence in Finnigan (2000), a collection of statistics about turbulence over plant canopies, the skewness of longitudinal and vertical velocity approach zero at twice the canopy top, which means that the turbulence at this height tends to be normally distributed just like a random noise with high frequency. In addition, the streamwise and vertical length scales of turbulence increase with height in that set of statistics, in agreement with the higher spectral peak of approximately 80 s for Pantanal, assuming a conversion between length and time using Taylor's hypothesis.

Table 2. Contribution of coherent structures to the heat flux (percentage). First row: cumulative sum for all frequencies; second row: cumulative sum from 10 to 200 s; third row: sum from range 10–200 s, but accounting only periods with stationarity of *T* signal within the top 10% of stationarity rate ($St\_T \geq 0.9$) for each site.

	Jaru	Pantanal	Manaus	Caxiuanã
Total	90.14	98.11	92.90	102.95
10–200 s	66.13	55.50	71.82	80.63
10–200 s (stationary)	76.57	56.85	82.28	84.33

The difference in cumulative flux between sites shown in the second row of Table 2 could be attributed to two factors: differences in the level of stationarity or simply differences among sites. The flow might be more or less disturbed by the canopy elements, topography or local circulations in each site, which in turn sets the stationarity to site-specific levels. To test these two possibilities, we selected only conditions when the stationarity rate exceeded the 90th percentile in each site and calculated the cumulative sum from 10–200 s, shown in the third row of Table 2. The result is that selecting only stationary periods in each site improved the fraction of the flux carried by coherent motions by 15% in Manaus and Jaru, but only 5% for Caxiuanã, which had already high levels of stationarity. This result shows the combined effect of differences among sites and the level of stationarity when accounting for the contribution of coherent motions to fluxes of heat.

5. Conclusions

The contribution of organized motions to the fluxes of heat, energy and scalars is variable from site to site, it

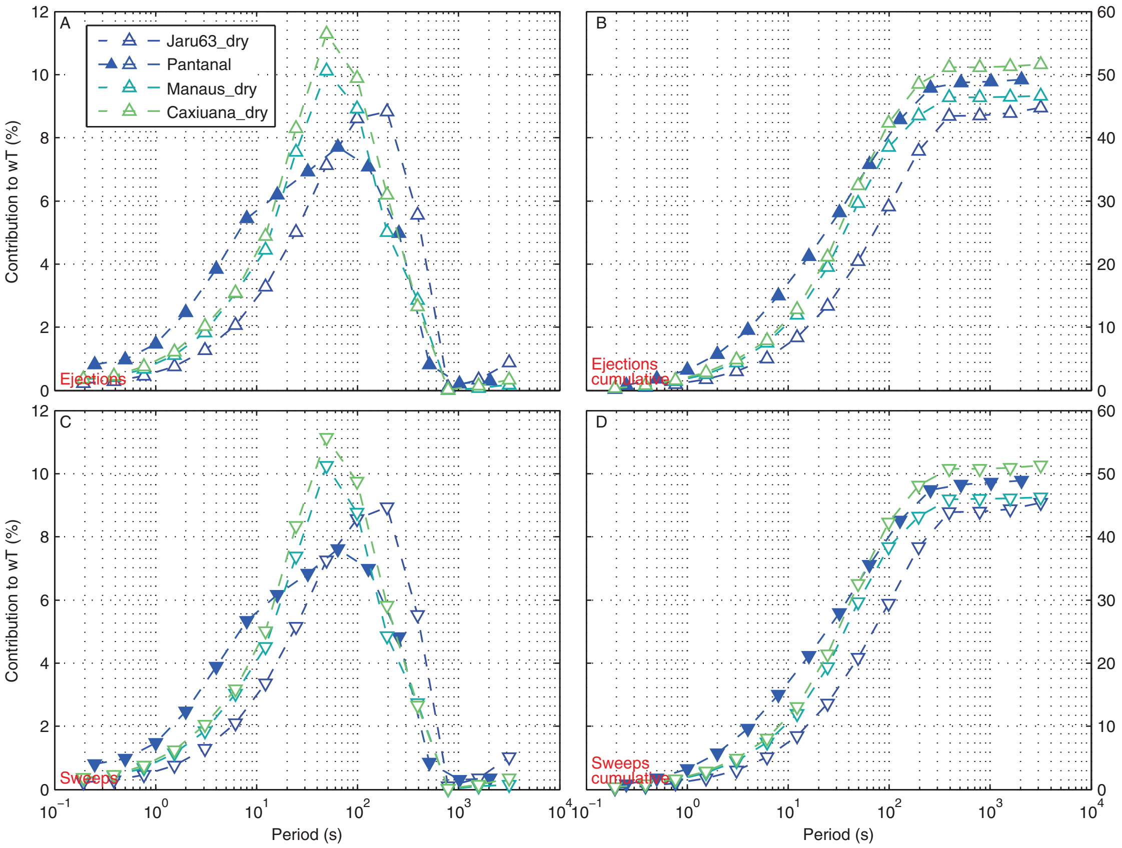

Figure 3. Contribution of ejections and sweeps to the daytime buoyancy heat flux. (a) Ejections, (b) cumulative ejections, (c) sweeps and (d) cumulative sweeps.

depends on the methodology used to detect the coherent motions, and it is also dependent on the definition of a coherent structure. In a previous work (Zeri and Sá, 2011a) it was reported that the typical period associated with coherent structures is determinant when accounting for their contribution to fluxes. Here, it was shown that an additional variable might be important when considering the contribution: the level of stationarity of time series used in the flux calculation, such as wind velocity components and air temperature. Considering only the forest sites used in this work, the site with the lowest levels of stationarity (Jaru) was the one with the lowest contribution of coherent motions to the buoyancy heat flux, when considering the sum from 10 to 200 s. The level of stationarity and the location of the peak contribution of organized motions are key factors when calculating how much of the flux is due to the coherent structures. In addition, not only site conditions influence the cumulative sum but also the level of stationarity. When very stationary periods were selected for each site the result was an increase in the contribution to fluxes of up to 15%. Several factors influence the results on the contribution of coherent structures to fluxes: the methodology used, the site conditions, the definitions of what is a coherent structure. Here, in this work, we contribute to this research by using the same methodology on multiple sites, resulting that the level of stationarity might also play a role when accounting for the impact of coherent motions on the fluxes.

Acknowledgements

M. Zeri is grateful to São Paulo Research Foundation (FAPESP) – grant 2011/04101-0 – for the support during the preparation of this manuscript. Leonardo Sá is particularly grateful to CNPq – *Conselho Nacional de Pesquisa e Desenvolvimento Tecnológico* – for his research grant (process 303.728/2010-8). For supporting the data collection at the Pantanal wetland and all forest sites, the authors are grateful to *Universidade Federal do Mato Grosso do Sul* (UFMS), *Centro de Previsão de Tempo e Estudos Climáticos* (CPTEC), *Instituto Nacional de Pesquisas Espaciais* (INPE) and the LBA project (Large Scale Biosphere-Atmosphere Experiment in the Amazon).

References

Andreae MO, Artaxo P, Brandao C, Carswell FE, Ciccioli P, da Costa AL, Culf AD, Esteves JL, Gash JHC, Grace J, Kabat P, Lelieveld J, Malhi Y, Manzi AO, Meixner FX, Nobre AD, Nobre C, Ruivo MDLP, Silva-Dias MA, Stefani P, Valentini R, von Jouanne J, Waterloo MJ. 2002. Biogeochemical cycling of carbon, water, energy, trace gases, and aerosols in Amazonia: the LBA-EUSTACH experiments. *Journal of Geophysical Research: Atmospheres* **107**: LBA 33-1–LBA 33-25.

Araujo AC, Nobre AD, Kruijt B, Elbers JA, Dallarosa R, Stefani P, von Randow C, Manzi AO, Culf AD, Gash JHC, Valentini R, Kabat P. 2002. Comparative measurements of carbon dioxide fluxes from two nearby towers in a central Amazonian rainforest: the Manaus LBA site. *Journal of Geophysical Research: Atmospheres* **107**: LBA 58-1–LBA 58-20.

de Araújo AC, Dolman AJ, Waterloo MJ, Gash JHC, Kruijt B, Zanchi FB, de Lange JME, Stoevelaar R, Manzi AO, Nobre AD. 2010. The

spatial variability of CO_2 storage and the interpretation of eddy covariance fluxes in central Amazonia. *Agricultural and Forest Meteorology* **150**: 226–237.
Bergstrom H, Hogstrom U. 1989. Turbulent exchange above a pine forest. 2. Organized structures. *Boundary-Layer Meteorology* **49**(3): 231–263.
Brunet Y, Irvine MR. 2000. The control of coherent eddies in vegetation canopies: streamwise structure spacing, canopy shear scale and atmospheric stability. *Boundary-Layer Meteorology* **94**(1): 139–163.
Cava D, Donateo A, Contini D. 2014. Combined stationarity index for the estimation of turbulent fluxes of scalars and particles in the atmospheric surface layer. *Agricultural and Forest Meteorology* **194**: 88–103.
Collineau S, Brunet Y. 1993. Detection of turbulent coherent motions in a forest canopy. 1. Wavelet analysis. *Boundary-Layer Meteorology* **65**(4): 357–379.
Conangla L, Cuxart J, Soler MR. 2008. Characterisation of the nocturnal boundary layer at a site in Northern Spain. *Boundary-Layer Meteorology* **128**(2): 255–276.
Daubechies I. 1992. *Ten Lectures on Wavelets*. CBMS-NSF Regional Conference Series in Applied Mathematics, 61. Society for Industrial and Applied Mathematics: Philadelphia, PA, 377 pp.
Dias Júnior CQ, Sá LDA, Pachêco VB, de Souza CM. 2013. Coherent structures detected in the unstable atmospheric surface layer above the Amazon forest. *Journal of Wind Engineering and Industrial Aerodynamics* **115**: 1–8.
Durden DJ, Nappo CJ, Leclerc MY, Duarte HF, Zhang G, Parker MJ, Kurzeja RJ. 2013. On the impact of wave-like disturbances on turbulent fluxes and turbulence statistics in nighttime conditions: a case study. *Biogeosciences* **10**: 8433–8443.
Farge M. 1992. Wavelet transforms and their applications to turbulence. *Annual Review of Fluid Mechanics* **24**: 395–457.
Finnigan J. 2000. Turbulence in plant canopies. *Annual Review of Fluid Mechanics* **32**: 519–571.
Foken T, Wichura B. 1996. Tools for quality assessment of surface-based flux measurements. *Agricultural and Forest Meteorology* **78**(1–2): 83–105.
Gao W, Shaw RH, Paw KT. 1989. Observation of organized structure in turbulent-flow within and above a forest canopy. *Boundary-Layer Meteorology* **47**(1–4): 349–377.
Hartmann DL. 1994. *Global Physical Climatology*. Academic Press: San Diego, CA, 425 pp.
Hogstrom U, Bergstrom H. 1996. Organized turbulence structures in the near-neutral atmospheric surface layer. *Journal of the Atmospheric Sciences* **53**(17): 2452–2464.
Kaimal JC, Finnigan JJ. 1994. *Atmospheric Boundary Layer Flows: Their Structure and Measurement*. Oxford University Press: New York, NY, 289 pp.
Kaimal JC, Gaynor JE. 1991. Another look at sonic thermometry. *Boundary-Layer Meteorology* **56**: 401–410.
Lee XH. 1998. On micrometeorological observations of surface-air exchange over tall vegetation. *Agricultural and Forest Meteorology* **91**(1–2): 39–49.
Li Q, Fu Z. 2013. The effects of non-stationarity on the clustering properties of the boundary-layer vertical wind velocity. *Boundary-Layer Meteorology* **149**(2): 219–230.
Liu HP, Foken T. 2001. A modified Bowen ratio method to determine sensible and latent heat fluxes. *Meteorologische Zeitschrift* **10**(1): 71–80.
Lu CH, Fitzjarrald DR. 1994. Seasonal and diurnal-variations of coherent structures over a deciduous forest. *Boundary-Layer Meteorology* **69**(1–2): 43–69.
Mahrt L. 1998. Flux sampling errors for aircraft and towers. *Journal of Atmospheric and Oceanic Technology* **15**(2): 416–429.
Mahrt L. 2011. The near-calm stable boundary layer. *Boundary-Layer Meteorology* **140**(3): 343–360.
Nogueira DS, Sá LDA, Cohen JCP. 2006. Rajadas noturnas e trocas de CO_2 acima da floresta de Caxiuanã, PA, durante a estação seca. *Revista Brasileira de Meteorologia* **21**(3b): 213–223.
von Randow C, Sa LDA, Gannabathula PSSD, Manzi AO, Arlino PRA, Kruijt B. 2002. Scale variability of atmospheric surface layer fluxes of energy and carbon over a tropical rain forest in southwest Amazonia – 1. Diurnal conditions. *Journal of Geophysical Research: Atmospheres* **107**: 1–12.
von Randow C, Kruijt B, Holtslag AAM. 2006. Low-frequency modulation of the atmospheric surface layer over Amazonian rain forest and its implication for similarity relationships. *Agricultural and Forest Meteorology* **141**(2–4): 192–207.
Raupach MR, Thom AS. 1981. Turbulence in and above plant canopies. *Annual Review of Fluid Mechanics* **13**: 97–129.
Raupach MR, Finnigan JJ, Brunet Y. 1996. Coherent eddies and turbulence in vegetation canopies: the mixing-layer analogy. *Boundary-Layer Meteorology* **78**(3–4): 351–382.
Sá LDA, Pacheco VB. 2006. Wind velocity above and inside Amazonian rain forest in Rondonia. *Revista Brasileira de Meteorologia* **21**(3a): 50–58.
Sá LDA, Sambatti SBM, Galvao GP. 1998. Applying the Morlet wavelet in a study of variability of the level of Paraguay River at Ladario, MS. *Pesquisa Agropecuária Brasileira* **33**: 1775–1785.
Schotanus P, Nieuwstadt FTM, Debruin HAR. 1983. Temperature-measurement with a sonic anemometer and its application to heat and moisture fluxes. *Boundary-Layer Meteorology* **26**(1): 81–93.
Spano D, Snyder RL, Duce P, Paw UKT. 2000. Estimating sensible and latent heat flux densities from grapevine canopies using surface renewal. *Agricultural and Forest Meteorology* **104**(3): 171–183.
Stull RB. 1988. *An Introduction to Boundary Layer Meteorology*. Kluwer Academic Publishers: Dordrecht, Netherlands, Boston, MA and London, 666 pp.
Thomas C, Foken T. 2005. Detection of long-term coherent exchange over spruce forest using wavelet analysis. *Theoretical and Applied Climatology* **80**(2–4): 91–104.
Thomas C, Foken T. 2007. Flux contribution of coherent structures and its implications for the exchange of energy and matter in a tall spruce canopy. *Boundary-Layer Meteorology* **123**(2): 317–337.
Thomas C, Martin JG, Goeckede M, Siqueira MB, Foken T, Law BE, Loescher HW, Katul G. 2008. Estimating daytime subcanopy respiration from conditional sampling methods applied to multi-scalar high frequency turbulence time series. *Agricultural and Forest Meteorology* **148**: 1210–1229.
Torrence C, Compo GP. 1998. A practical guide to wavelet analysis. *Bulletin of the American Meteorological Society* **79**(1): 61–78.
Vickers D, Mahrt L. 1997. Quality control and flux sampling problems for tower and aircraft data. *Journal of Atmospheric and Oceanic Technology* **14**(3): 512–526.
Wallace JM, Eckelmann H, Brodkey RS. 1972. The wall region in turbulent shear flow. *Journal of Fluid Mechanics* **54**(01): 39–48.
Webb EK, Pearman GI, Leuning R. 1980. Correction of flux measurements for density effects due to heat and water-vapor transfer. *Quarterly Journal of the Royal Meteorological Society* **106**(447): 85–100.
Wilczak JM, Oncley SP, Stage SA. 2001. Sonic anemometer tilt correction algorithms. *Boundary-Layer Meteorology* **99**(1): 127–150.
Wilks DS. 1995. *Statistical Methods in the Atmospheric Sciences: An Introduction*, Vol. **59**. Academic Press: San Diego, CA, 467 pp.
Zeri M, Sá LDA. 2011a. Scale dependence of coherent structures' contribution to the daytime buoyancy heat flux over the Pantanal wetland, Brazil. *Atmospheric Science Letters* **12**(2): 200–206. [Correction added on 31 December 2014 after original online publication: the reference Zeri and Sá 2011b has been removed since it was a duplication of Zeri and Sá 2011a.]
Zeri M, Sá LDA. 2011c. Horizontal and vertical turbulent fluxes forced by a gravity wave event in the nocturnal atmospheric surface layer over the Amazon forest. *Boundary-Layer Meteorology* **138**(3): 413–431.
Zeri M, Sá LDA, Nobre CA. 2013. Estimating buoyancy heat flux using the surface renewal technique over four Amazonian forest sites in Brazil. *Boundary-Layer Meteorology* **149**(2): 179–196.